

A Modified MWPM Decoding Algorithm for Quantum Surface Codes Over Depolarizing Channels

Yaping Yuan

*Department of Electrical Engineering
National Tsing Hua University
Hsinchu 30013, Taiwan
yapingyuan@mx.nthu.edu.tw*

Chung-Chin Lu

*Department of Electrical Engineering
National Tsing Hua University
Hsinchu 30013, Taiwan
cclu@ee.nthu.edu.tw*

Abstract—Quantum Surface codes are a kind of quantum topological stabilizer codes whose stabilizers and qubits are geometrically related. Due to their special structures, surface codes have great potential to lead people to large-scale quantum computation. In the minimum weight perfect matching (MWPM) decoding of surface codes, the bit-flip errors and phase-flip errors are assumed to be independent for simplicity. However, these two kinds of errors are likely to be correlated in the real world. In this paper, we propose a modification to MWPM decoding for surface codes to deal with the noises in depolarizing channels where bit-flip errors and phase-flip errors are correlated. With this modification, we obtain thresholds of 17% and 15.3% for the surface codes with mixed boundaries and the surface codes with a hole, respectively.

Index Terms—Quantum error-correcting codes, surface codes, topological codes, quantum computing.

I. INTRODUCTION

To reduce the impact of noises in quantum computing systems, quantum error-correcting codes play a very important role in the development of quantum computation. Stabilizer codes are a class of quantum error-correcting codes that have a strong connection with classical error-correcting codes. The code space of a stabilizer code is determined by the so-called stabilizers. Topological codes are a type of stabilizer codes whose stabilizers and data qubits have a geometrical or topological relation. Due to their special structures, it is believed that topological codes have great potential to be implemented on a large scale. Therefore, they have gained a lot of attention in recent years. Topological codes evolved from Alexei Kitaev's invention known as toric codes [1], in which qubits are distributed on the surface of a torus. Planar versions were brought later, and are called surface codes [2], [3].

Many different decoders for surface codes have been developed in recent years, such as the decoders based on belief-propagation (BP) [4], [5], union-find (UF) [6], [7], and matrix product states (MPS) [8]. The most standard decoder of surface codes is the minimum weight perfect matching (MWPM) decoder. When the bit-flip errors and the phase-flip errors are assumed to be uncorrelated, the quantum maximum likelihood

decoding (QMLD) of surface codes can be reduced to the problem of finding the minimum weight perfect matching on a graph. But in fact, the depolarizing noise model, where the bit-flip errors and the phase-flip errors are correlated, is closer to the real world. In this paper, we propose a modification to the conventional MWPM decoding for surface codes to deal with the noises in depolarizing channels.

Our method is based on iteratively reweighting the dual lattice and the primal lattice by the correction patterns on each other lattice. A similar method is proposed in [11], where it is not shown whether this method can guarantee that the weight of the correction operation will never increase along the iterations. In this paper, besides showing how the iteratively reweighted MWPM decoding works, we will also give a proof to show that the weight of the correction operation will never increase along the iterations.

This paper is organized as follows. In Section II, we will review the structure of surface codes and introduce the MWPM decoder. In Section III, we will discuss our modification to the MWPM decoder. In Section IV, we will present the simulation results. Section V concludes this paper.

II. BASICS OF SURFACE CODES

A. Structure of Surface Codes

In this paper, we will use a way similar to [12] to describe a surface code. A surface code is defined on a square lattice and every edge on this lattice is associated with a qubit. There are two types of stabilizer generators: plaquette stabilizer generators and vertex stabilizer generators. Every plaquette is associated with a plaquette stabilizer generator. A plaquette stabilizer generator consists of a tensor product of Pauli Z operators acting on the qubits which lie on the plaquette's boundary, as illustrated in Fig. 1(a). For every vertex, there is a vertex stabilizer generator which consists of a tensor product of Pauli X operators acting on the qubits adjacent to the vertex, as shown in Fig. 1(b).

There are two main types of surface codes, one is built on a lattice with mixed boundaries [2], and the other is built on a lattice with holes (or defects) [3]. As shown in Fig.

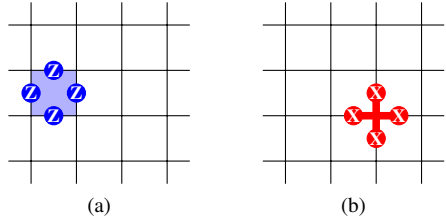


Fig. 1. (a) A plaquette operator (b) A vertex operator.

2(a), surface codes with mixed boundaries are constructed on a lattice surrounded by two pairs of different boundaries. And as shown in Fig. 2(b), surface codes with a hole are constructed on a lattice where a plaquette stabilizer generators in the middle of the lattice are removed. Note that the size of a hole is not necessarily 1×1 . In Fig. 2, the original lattice is called the primal lattice, and the lattice depicted in dashed line is called the dual lattice [12].

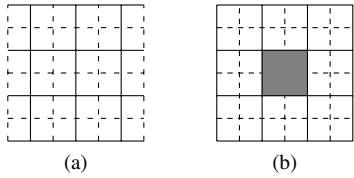


Fig. 2. (a) A surface code with mixed boundaries. (b) A surface code with a hole.

B. Syndromes of Surface Codes

For a stabilizer code, each stabilizer generator corresponds to an element of the syndrome vector. For an error E , the stabilizer generators which anti-commute with E will give a 1 in the syndrome vector, otherwise 0. In a surface code, for simplicity, we call the stabilizer generators that produce nonzero elements in the syndrome vector as ‘‘syndrome nodes’’.

Suppose E_Z is a tensor product of Pauli Z errors. Since a Pauli X anti-commutes with a Pauli Z , if we express E_Z as strings on the primal lattice, then the syndrome nodes corresponding to E_Z are the endpoints of those strings, as shown in Fig. 3(a). Similarly, for X -type errors, we can express them as strings on the dual lattice, then the syndrome nodes corresponding to those X -type errors are the endpoints of those strings, as shown in Fig. 3(b). Since a Pauli Y anti-commute with both a Pauli X and a Pauli Z , we can treat a Y error as a combination of an X error and a Z error.

For a surface code with a hole, operators that commute with all stabilizers but not stabilizers themselves are either loops of Z operators that wind around the hole or strings of X operators that connect the inner and outer boundaries. Thus, let the number of qubits on the shortest path between the inner boundary and the outer boundary be d_b and the number of qubits around the hole be d_h , the code distance of a surface code with a hole is $d = \min(d_b, d_h)$. Therefore, the distance of the surface code in Fig. 2(b) is 2. For a surface code with mixed boundaries, its code distance is the distance between the two sides. Hence the code distance of Fig. 2(a) is 4.

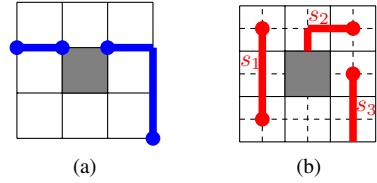


Fig. 3. (a) A tensor product of Z errors is depicted in blue lines and the corresponding syndrome nodes are depicted in blue circles. (b) A tensor product of X errors is depicted in red lines and the corresponding syndrome nodes are depicted in red circles. The string s_1 has two plaquette generators which anti-commute with it, but s_2 and s_3 both have only one plaquette operator which anti-commutes with them.

C. MWPM decoding of Surface Codes

Since the syndrome of a surface code can be viewed as nodes on the primal lattice and the dual lattice, the quantum maximum likelihood decoding can be reduced to the problem that finds the most likely string patterns with the same syndrome nodes [9]. How to choose the most likely correction strings depends on the noise models.

Suppose that X errors and Z errors are independent and a Y error is considered as a combination of an X error and a Z error, then we can decode X errors and Z errors separately. To decode Z errors only, we just need to find the strings on the primal lattice with the minimum weight such that connect all the syndrome nodes on the primal lattice. For the decoding of the X type errors, it’s similar, but the lattice we are working on is the dual lattice. Therefore, the decoding of a surface code can be regarded as two minimum weight perfect matching problems. Although the number of syndrome nodes may be odd, with some modifications, the decoding problem can still be reduced to a MWPM problem. The noise model where X errors and Z errors are independent to each other is called the uncorrelated noise model. To solve a MWPM problem, there is a well-known algorithm developed by Jack Edmonds, known as the blossom algorithm [10]. For a graph $G = (V, E)$, the time complexity of the blossom algorithm is $O(|V|^3)$, therefore, for an $L \times L$ lattice, the the complexity of the MWPM decoder is $O(L^6)$.

III. ITERATIVELY REWEIGHTED MWPM DECODING OF SURFACE CODES

The depolarizing noise model is the most considered noise model in quantum error-correction. In depolarizing channels, each qubit has the probability of $1 - \epsilon$ to remain untainted, and has the probability of $\frac{\epsilon}{3}$ to be affected by X , Y , and Z , respectively. Therefore, in depolarizing channels, if we view a Y error as a combination of X and Z , then the conditional probability $P(X|Z) = 0.5$, so X errors and Z errors are not independent to each other.

As shown in Fig. 4(a), let the small circles be the syndrome nodes, if we use the MWPM decoding, then we will get this decoding result. But if the noise model we are considering is the depolarizing noise model, then the decoding result of QMLD should be Fig. 4(b).

In Fig. 4(a), we have 4 X operators and 4 Z operators, so the total weight of this correction is 8. In Fig. 4(b), although

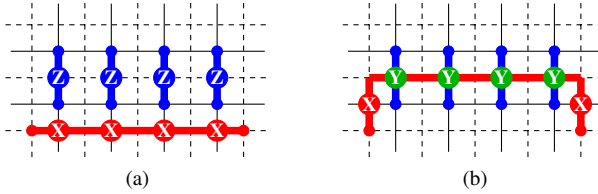


Fig. 4. The QMLD over (a) the uncorrelated noise model and (b) the depolarizing noise model.

it has 6 X operators and 4 Z operators, under the view point of depolarizing noise model, we have 4 Y and 2 X . Since the total weight in Fig. 4(b) is only 6, it is a better choice than Fig. 4(a) when the noise model is the depolarizing noise model.

Here we can find that when the correction strings on the primal lattice is fixed, if a string on the dual lattice touches a string on the primal lattice, the intersection won't increase the total weight, since it just turns a single Z correction into a single Y correction. Therefore the shortest path from one syndrome node on the dual lattice to another is not necessarily the string that can minimize the total weight.

However, if we reweight the edges on the dual lattice that touches the correction strings on the primal lattice to 0, the shortest path between the two syndrome nodes on the reweighted dual lattice is the correction string that causes the least extra total weight. As shown in Fig. 5, the shortest path between the two syndrome nodes on the reweighted dual lattice is now P_2 instead of P_1 . Therefore, when the correction of Z -type error is fixed, finding the MWPM on the reweighted dual lattice can give us the error pattern that minimizes the total weight.

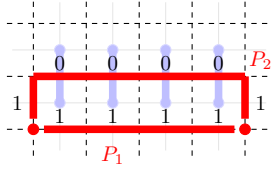


Fig. 5. The reweighted dual lattice.

Since the Z correction in a QMLD may not be a MWPM on the primal lattice, we can repeat this process more than one times to give us a better decoding result. We can use the MPWM on the reweighted dual lattice to reweight the primal lattice with the similar way, and then use the new MWPM on the reweighted primal lattice to reweight the original dual lattice again. In this paper, we will prove that no matter how many times we repeat this reweighting process, the total weight will never increase and it will remain the same or become smaller and smaller.

Let \mathcal{P}_0 be the original primal lattice and \mathcal{D}_0 be the original dual lattice. Let B_0 be a MWPM on \mathcal{P}_0 and R_0 be a MWPM on \mathcal{D}_0 . We reweight \mathcal{D}_0 with B_0 and call it the first reweighted dual lattice \mathcal{D}_1 . Let R_1 be a MWPM on \mathcal{D}_1 . We reweight \mathcal{P}_0 with R_1 and call it the first reweighted primal lattice \mathcal{P}_1 . We

can use the similar way to construct B_k and R_k , $k \in \mathbb{N}$. Note that for $i > 0$, \mathcal{D}_i is constructed by reweighting \mathcal{D}_0 with B_{i-1} and \mathcal{P}_i is constructed by reweighting \mathcal{P}_0 with R_i .

When we have gotten B_i and R_i and try to calculate the total weight of them, we can not just calculate the weights of B_i and R_i both on the reweighted lattices and sum them up. One of them must be calculated on the original lattice and the other is calculated on the reweighted lattice reweighted by the first matching. Since \mathcal{P}_i is constructed based on R_i , to calculate the total weight of B_i and R_i , we can calculate the weight of R_i on \mathcal{D}_0 first, and calculate that of B_i on \mathcal{P}_i , and then sum them up.

Let the weight of a matching M on the i th reweighted lattice as $W_i(M)$. We can define the i th total weight as

$$T_i = W_i(B_i) + W_0(R_i), \quad i \geq 1.$$

For the case $i = 0$, we need a different definition, since $W_0(B_0)$ is clearly not the weight of B_0 on the lattice reweighted by R_0 . But since \mathcal{D}_1 is the lattice reweighted by B_0 , we can sum the weight of B_0 on \mathcal{P}_0 and that of R_0 on \mathcal{D}_1 . Thus, the total weight of B_0 and R_0 is

$$T_0 = W_0(B_0) + W_1(R_0).$$

And example of the modified decoding process and examples of the above definitions can be seen in Fig. 6.

Theorem 1. $T_i \leq T_{i-1}$ for all $i \in \mathbb{N}$.

Proof. For a MWPM M_P on the primal lattice and a MWPM M_D on the dual lattice, there are two ways to calculate the total weight. The first one is summing the weight of M_P on the original primal lattice and the weight of M_D on the dual lattice reweighted by M_P . The second one is the reverse, i.e., summing the weight of M_D on the original dual lattice and the weight of M_P on the primal lattice reweighted by M_D . Therefore, for $i \geq 1$, we have the following properties

$$W_0(B_{i-1}) + W_i(R_i) = W_i(B_{i-1}) + W_0(R_i) \quad (1)$$

$$W_i(B_i) + W_0(R_i) = W_0(B_i) + W_{i+1}(R_i). \quad (2)$$

Since the definition of T_i are different for $i = 0$ and $i \geq 1$, we need to discuss two cases. For $i = 1$, since R_1 is a MWPM on \mathcal{D}_1 , we have $W_1(R_1) \leq W_1(R_0)$, then

$$W_0(B_0) + W_1(R_1) \leq W_0(B_0) + W_1(R_0) = T_0.$$

Since $W_0(B_0) + W_1(R_1) = W_1(B_0) + W_0(R_1)$, we have

$$W_1(B_0) + W_0(R_1) \leq W_0(B_0) + W_1(R_0) = T_0.$$

Since B_1 is a MWPM on \mathcal{P}_1 , we have $W_1(B_1) \leq W_1(B_0)$. Therefore,

$$T_1 = W_1(B_1) + W_0(R_1) \leq W_0(B_0) + W_1(R_0) = T_0.$$

For $i \geq 2$, starting from $T_{i-1} = W_{i-1}(B_{i-1}) + W_0(R_{i-1})$, by Equation 2, we have $T_{i-1} = W_0(B_{i-1}) + W_i(R_{i-1})$. Since R_i is a MWPM on \mathcal{D}_i , we have

$$W_0(B_{i-1}) + W_i(R_i) \leq W_0(B_{i-1}) + W_i(R_{i-1}) = T_{i-1}.$$

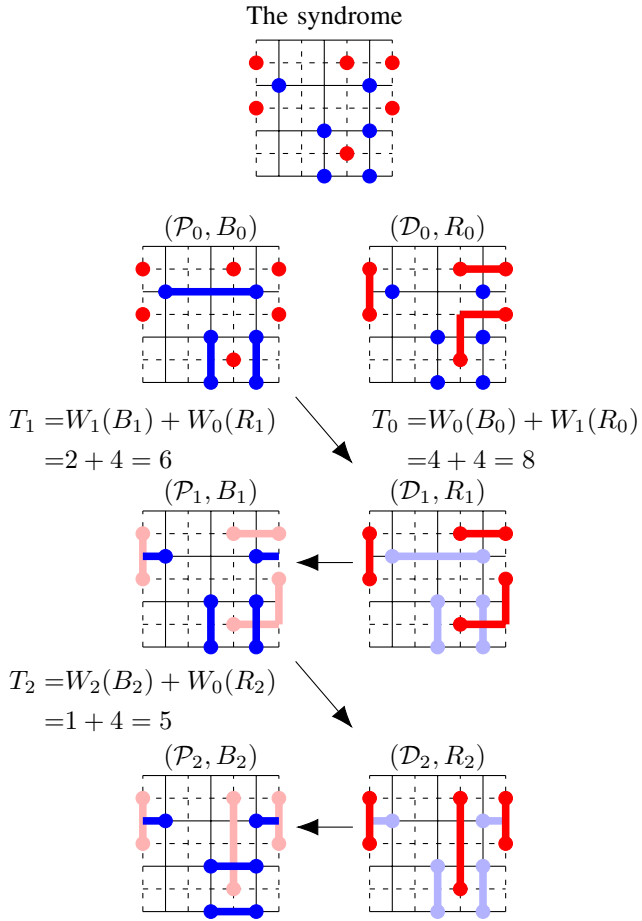


Fig. 6. An example of the modified decoding process.

By Equation 1, we have

$$W_0(B_{i-1}) + W_i(R_i) = W_i(B_{i-1}) + W_0(R_i).$$

Similarly, since B_i is a MWPM on \mathcal{P}_i , we have $W_i(B_i) \leq W_i(B_{i-1})$. Then,

$$T_i = W_i(B_i) + W_0(R_i) \leq W_i(B_{i-1}) + W_0(R_i) \leq T_{i-1}.$$

□

Here we need to indicate that this modification does not guarantee the minimum total weight result. Take Fig. 4 as an example. If the MWPM we find on the primal lattice is as Fig. 7, then this method will fail to give the correction pattern with minimum total weight.

In Section II, we do not discuss the time complexity of constructing the syndrome node graph, since the shortest path of any two syndrome nodes can be obtained in $O(1)$. But on the reweighted lattice, the shortest path between two syndrome nodes is not that clear. To find the shortest paths between all pairs of nodes in a graph, we can use Floyd-Warshall algorithm or use Dijkstra's algorithm on each pair of nodes. For a graph with n nodes, the time complexity is $O(n^3)$ for both methods,

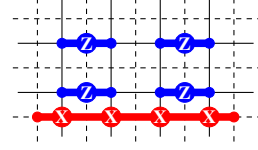


Fig. 7. For the syndrome in Fig. 4, if Z -type errors are decoded as this, then this algorithm won't give us the correction pattern with minimum total weight. It's an example shows that the IRMWPM decoder doesn't guarantee the results of maximum likelihood decoding over depolarizing channel.

therefore, the time complexity of constructing the syndrome node graph is $O(n^3)$.

As we will see in Section IV, numerically, for lattices with size smaller than 30×30 , the numbers of iteration needed are rarely more than 5. Hence, we can neglect it in the calculation of the total time complexity. Therefore, the time complexity for the IRMWPM decoder is still $O(n^3)$.

IV. SIMULATION RESULTS

Since we will repeat the same process more than one time, we need to set a stopping criterion. Note that if for any two same complete graphs G_1 and G_2 , the MWPM subroutine we use will give us the same results, then we can use whether there is a previous correction pattern B_i or R_i is the same as the current one as the stopping criterion.

Here, we show that the decoding performance of three different cases. In the first one, we only apply MWPM decoding without any reweighting to the lattices. In the second one, we reweight the dual lattice only one time, i.e., use B_0 and R_1 as the correction. In the third one, the looping will continue until the new MWPM is the same as one of the previous MWPMs.

As we can see in Fig. 8, if we reweight the lattice only one time, the improvement of decoding performance becomes less and less as the qubit error rate goes smaller and smaller. But if we use the stopping criterion we mentioned above, the improvement of the decoding performance is very obvious.

Now we want to know how many times do we need to repeat this reweighting process. Empirically, it is rarely over 5 when the size of the lattice is smaller than 30×30 and the qubit error rate is less than 0.1. The counting of the extra iterations starts from using B_1 to reweight the dual lattice. Since the stopping criterion cannot be triggered without B_1 , using B_0 to reweight the dual lattice and using R_1 to reweight the primal lattice will not be counted as extra iterations. Fig. 9 shows the distribution of how many extra iterations do the surface codes with mixed boundaries need for different code distances.

For a surface code, we may want to increase the size of the lattice to lower the logical error rate. But the larger the lattice is, the more errors may be introduced into the system and the logical error rate will increase. The error probability over which the logical error rate will increase as the size of the code gets larger is called the threshold. As shown in Fig. 10, for the surface codes with mixed boundaries, if the decoder is the MWPM decoder, the threshold is about 15.5%, but if the decoder is IRMWPM decoder, then the threshold can be

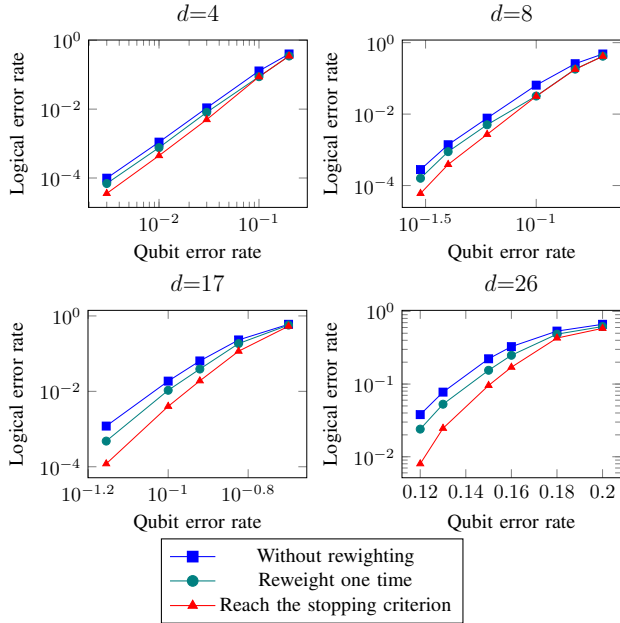


Fig. 8. The decoding simulation of the surface codes with mixed boundaries.

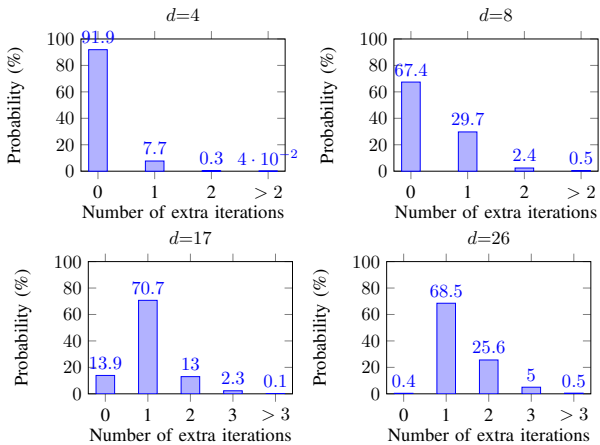


Fig. 9. The distribution of how many extra iterations do surface codes with mixed boundaries need when the qubit error rate is 0.1. The average of these four cases are 0.08, 0.34, 1.04, and 1.32, respectively.

increased to approximately 17%. For surface codes with a hole, if we don't apply any reweighting, the threshold is about 14.2%, but if the decoder is the IRMWPM decoder, then the threshold is approximately 15.3%, as shown in Fig. 11.

V. CONCLUSION

We propose a modification to the conventional MWPM decoding of surface codes to deal with the noises in depolarizing channels where the bit-flip errors and the phase-flip errors are correlated. Our method is mainly based on repeatedly using the MWPM on one lattice to reweight the other lattice to get a correction pattern with possibly less total weight. In this paper, we prove that the total weight will never increase when we repeat this reweighting process. And we present the simulation

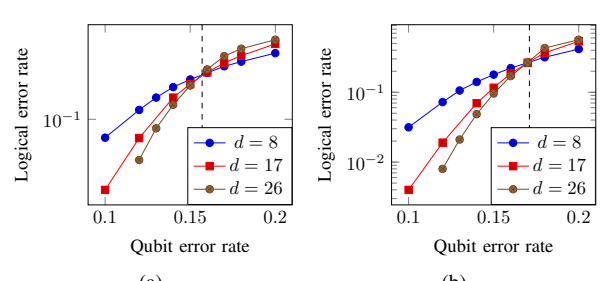


Fig. 10. Decoding performance of (a) MWPM decoder and (b) IRMWPM decoder on the surface codes with mixed boundaries.

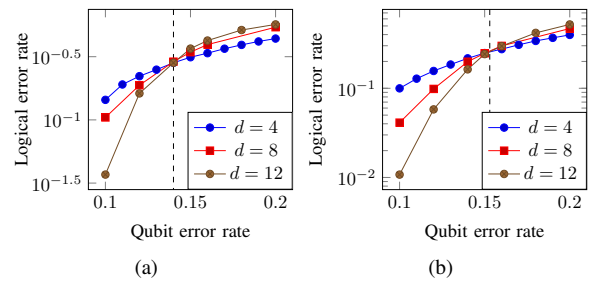


Fig. 11. Decoding performance of (a) MWPM decoder and (b) IRMWPM decoder on the surface codes with a hole.

results of both the surface codes with mixed boundaries and the surface codes with a hole to show the improvement of the decoding performance.

REFERENCES

- [1] A. Y. Kitaev, "Fault-tolerant quantum computation by anyons," *Annals of Physics*, vol. 303, no. 1, pp. 2–30, 2003.
- [2] S. B. Bravyi and A. Y. Kitaev, "Quantum codes on a lattice with boundary," *arXiv preprint quant-ph/981052*, 1998.
- [3] M. H. Freedman and D. A. Meyer, "Projective plane and planar quantum codes," *Foundations of Computational Mathematics*, vol. 1, no. 3, pp. 325–332, 2001.
- [4] K.-Y. Kuo and C.-Y. Lai, "Refined belief propagation decoding of sparse-graph quantum codes," *IEEE J. Sel. Area. Inf. Theory*, vol. 1, no. 2, pp. 487–498, 2020.
- [5] B. Criger and I. Ashraf, "Multi-path Summation for Decoding 2D Topological Codes," *Quantum*, vol. 2, pp. 102, 2018.
- [6] N. Delfosse and N. H. Nickerson, "Almost-linear time decoding algorithm for topological codes," *arXiv preprint arXiv:1709.06218*, 2017.
- [7] S. Huang, M. Newman, and K. R. Brown, "Fault-Tolerant Weighted Union-Find Decoding on the Toric Code," *Physical Review A*, vol. 102, no. 012419, 2020.
- [8] S. Bravyi, M. Suchara, and A. Vargo, "Efficient algorithms for maximum likelihood decoding in the surface code," *Phys. Rev. A*, vol. 90, no. 032326, 2014.
- [9] K. Y. Kuo, "On the encoding and decoding complexities of quantum stabilizer codes," Ph.D. dissertation, National Tsing Hua University, 2015.
- [10] J. Edmonds, "Paths, trees, and flowers," *Canadian Journal of mathematics*, vol. 17, pp. 449–467, 1965.
- [11] A. G. Fowler, "Optimal complexity correction of correlated errors in the surface code," *arXiv preprint arXiv:1310.0863*, 2013.
- [12] H. Bombín, "Topological codes," in *Quantum Error Correction*, D. A. Lidar and T. A. Brun, Eds., 1st ed. Cambridge: Cambridge University Press, 2013.
- [13] A. G. Fowler, M. Mariantoni, J. M. Martinis, and A. N. Cleland, "Surface codes: Towards practical large-scale quantum computation," *Physical Review A*, vol. 86, no. 032324, 2012.